Supplemental Document

Biomedical Optics EXPRESS

SpeCamX: mobile app that turns unmodified smartphones into multispectral imagers: supplement

Qinghua He,[1,2,†] Wanyu Li,[3,†] Yaping Shi,[2] Yi Yu,[1] Wenqian Geng,[3] Zhiyuan Sun,[1,5] and Ruikang K. Wang[2,4,6,]

[1]*Changchun Institute of Optics, Fine Mechanics and Physics, Chinese Academy of Science, Changchun, Jilin 130033, China*
[2]*Department of Bioengineering, University of Washington, Seattle, Washington 98105, USA*
[3]*Department of Hepatobiliary and pancreatic Medicine, The first Hospital of Jilin University NO.71 Xinmin Street, Changchun, Jilin 130021, China*
[4]*Department of Ophthalmology, University of Washington, Seattle, Washington 98109, USA*
[5]*sunzhiyuan@ciomp.ac.cn*
[6]*wangrk@uw.edu*
[†]*These authors contributed equally to this work*

Supplement DOI: https://doi.org/10.6084/m9.figshare.23954856

Parent Article DOI: https://doi.org/10.1364/BOE.497602

Supplementary Material

SpeCamX: Mobile app that turns unmodified smartphones into multispectral imagers

Qinghua He,[1,2,†] Wanyu Li,[3,†] Yaping Shi,[2] Yi Yu,[1] Wenqian Geng,[3] Zhiyuan Sun,[1,*] and Ruikang Wang[2,4,*]

[1]*Changchun Institute of Optics, Fine Mechanics and Physics, Chinese Academy of Science, Changchun, Jilin 130033, China*
[2]*Department of Bioengineering, University of Washington, Seattle, Washington 98105, USA*
[3]*Department of Hepatobiliary and pancreatic Medicine, The first Hospital of Jilin University NO.71 Xinmin Street, Changchun, Jilin 130021, China*
[4]*Department of Ophthalmology, University of Washington, Seattle, Washington 98109, USA*
[†] *These authors contributed equally to this work.*
* *wangrk@uw.edu.*

Section 1. Workflow of SpeCamX

"Imager" fragments

The subject is labeled from the left top of the interface, which is auto saved with time stamp in the filename of acquired data cubes for further references. With different illumination conditions, we provided several options to set up the camera (see main text Fig. 2B). The default condition is to use built-in flashlight to illuminate subject. In this case, users can select their smartphone models in the "PHONE MODEL" option under the drop-down menu of settings. In this option, we pre-stored transformation matrices (TMs) to support a variety of smartphone models. Therefore, users can invoke corresponding matrices by simply selecting the smartphone model they use. As long as it is in dark environment, it is ready to go. In our clinical imaging test, the data were acquired using this setup.

In addition to the default setting, there are a number of other options for users to select if the requirement for default setting is not met, for example the smartphone that is in use is not supported or the environment is not in dark condition. Under these circumstances, the user can generate a customized TM on site through a self-recalibration step. In doing so, the user needs to first tap the "COLOR CHART" icon, in which there are provided with two options, i.e. either to use "24 blocks" or "96 blocks" to build the TM matrix (see main text Fig. 2B). Here, we used X-rite ColorChecker as the default color standard example for recalibration. The "24 blocks" option is provided for color charts with 24 classic color series. The available products include *X-rite ColorChecker Classic/Passport/Mini/Nano* (Fig. S1). The "96 blocks" option works for *X-rite ColorChecker Digital SG* which includes expanded 96 color blocks with standard reflectance spectrums (Fig. S2). After selecting the color chart option, the user can tap into a calibration page and sample the on-site color chart by tapping the camera icon. In this page, a box array would be generated to guide the sampling of color blocks. For example, in the page of "24 blocks", a six by four green box array would appear on the interface (see main text Fig. 2C). By pressing the photo button, the averaged RGB values in these boxes would be collected to compute a new TM with their reflectance spectra. During the calibration, the RGB values can be previewed on the top of corresponding boxes to prevent overexposure. The procedures for "96 blocks" option are the same but the box array is set to be twelve by eight.

Furthermore, even under an illumination that cannot be controlled or stabilized, there is provided another option to perform real-time recalibration in the "COLOR CHART" tap, which is termed "co-illumination" strategy. In the "co-illumination", the color charts and subjects will have to be placed within the same field of view for imaging, which will guarantee a shared illumination condition between the calibration and testing data cubes (Fig. S3). For this purpose, we can manually adjust the relative positions and sizes of the sampling box array to avoid the overlap between the color chart and the subject in the field of view. This strategy is suitable for trials if it is not possible to control the illumination environment, for example in the outdoor environment.

Except for on-site imaging, users can also load previous or external data by tapping the "Add data" icon on the top of the interface. The acquired and uploaded data can be labeled with "C" and "T", representing data for color charts and subjects, respectively. In this case, every smartphone installed with SpeCamX can act as a processing platform for an external data set.

"Records" fragments

The data specific to a subject can be recalled and reviewed by selecting that subject or sliding the drop-down menu up and down to check the thumbnails. To edit the data, several operations, including "Delete", "Calibration", "MSI" and "Analysis" are offered by long clicking. "Calibration" is provided for color chart data labeled with "C" to calculate a new TM. Tapping "MSI" and "Analysis" can switch to the corresponding fragments to show the related information of the selected case.

"MSI" fragments

The grayscale images at wavelengths from 420 to 680 nm are presented in a scrolling display started with the corresponding RGB photograph (Fig. S4). The wavelength is labeled on the top of each spectral image concurrently.

"Analysis" fragments

The BBL estimation results would be mapped in the "Bili" page, where a green box would guide the users to select a ROI. The averaged reflectance spectrum from the ROI would be read out that provides the prediction of BBL.

Considering the complexity of clinical imaging, we provided enough flexibility for the sampling procedure. The size of the ROI can be set in the "AVERAGE PIXELS" option (Fig. S5) and its position can be manually shifted to the desired regions of interest. (Fig. S6). Averaged RGB values in the ROI is shown in display so that the user can check to make sure the region is not overexposed. The shown "BILI" value represents the prediction made by the reflectance spectrum averaged from the ROI. The spectrum and predicted BBL are saved by tapping the photo icon for later use.

Except for the prediction of BBL (Bili) used in this study, SpeCamX also integrated algorithms to map other features like blood perfusion (Hemo), melanin pigmentation (Mela) and et al. Users can launch these functions by switching analysis algorithms from the drop-down menu on the top of the interface.

Fig. S1. Interfaces of the "24 blocks" and "96 blocks" calibration pages and compatible color charts for these options. (**A**) "24 blocks" option for 24 classic colors. A 6 by 4 box array was previewed to guide the sampling of RGB values. The RGB values were previewed on the top of the sampling box. Standard color charts with 24 classic colors, like *X-rite ColorChecker Classic/ Passport/ Classic Mini/ Classic Nano*, can be used in this option. (**B**) "96 blocks" option for expanded colors. A twelve by eight box array was previewed to guide the sampling of RGB values. *X-rite ColorChecker Digital SG* can be used in this option.

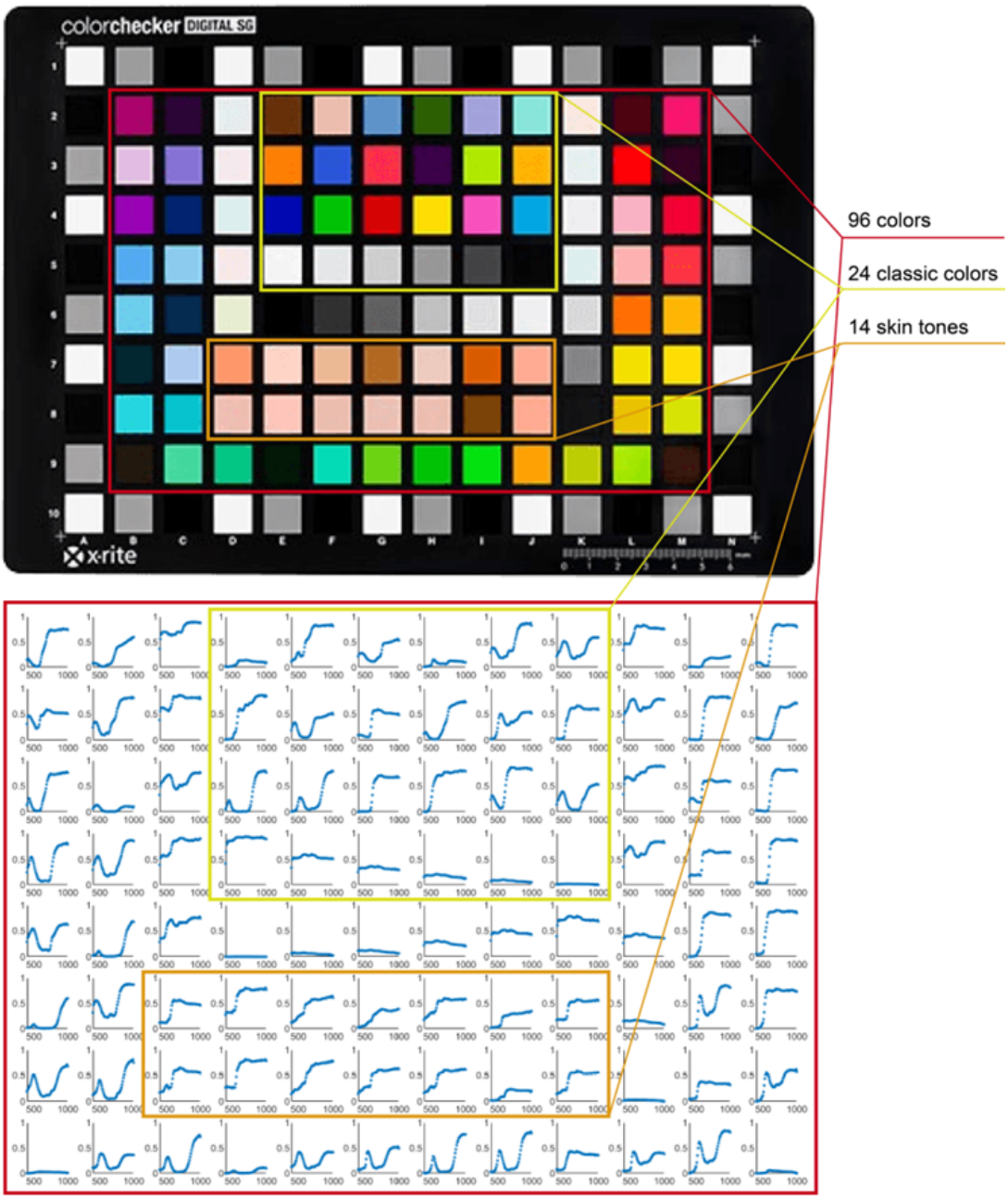

Fig. S2. Reflectance spectrums of 96 color blocks in *X-rite ColorChecker Digital SG*.

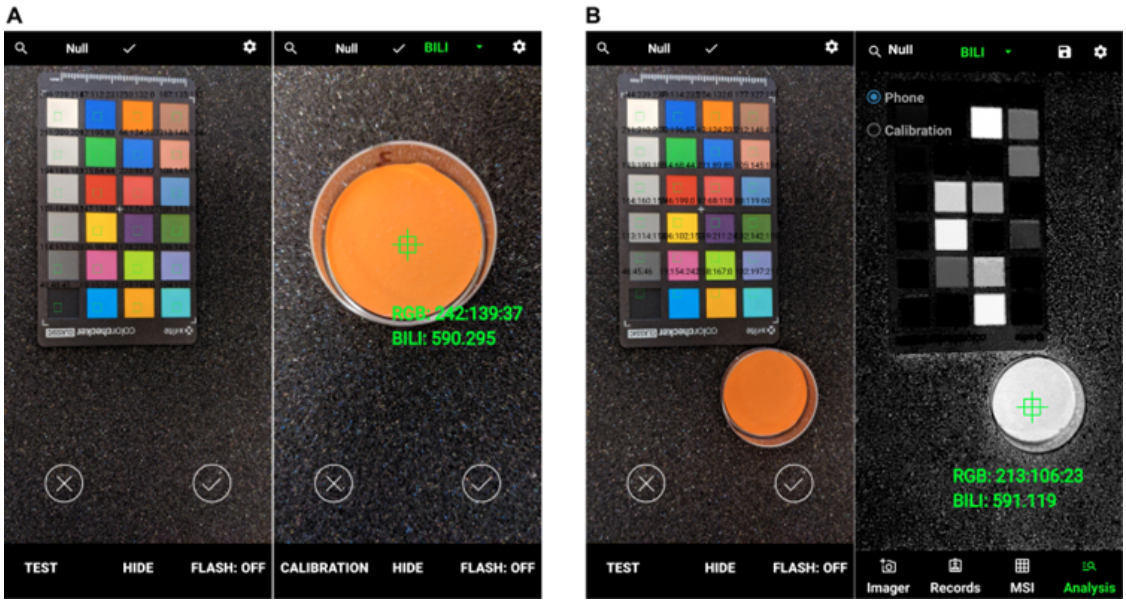

Fig. S3. Recalibration under uncontrolled and instable illumination. While the external illumination source cannot be controlled and stabilized, users can adopt a "co-illumination" step to realize real-time calibration. Instead of separately conducting "Calibration" and "Test" (A) the subject would be imaged with the color chart together in "Calibration". To do this, the box array would be rescaled to make space for the subject (B). The prediction results would be presented in the "Analysis" fragment. Please also see Visualization 1 (Movie S1.mp4).

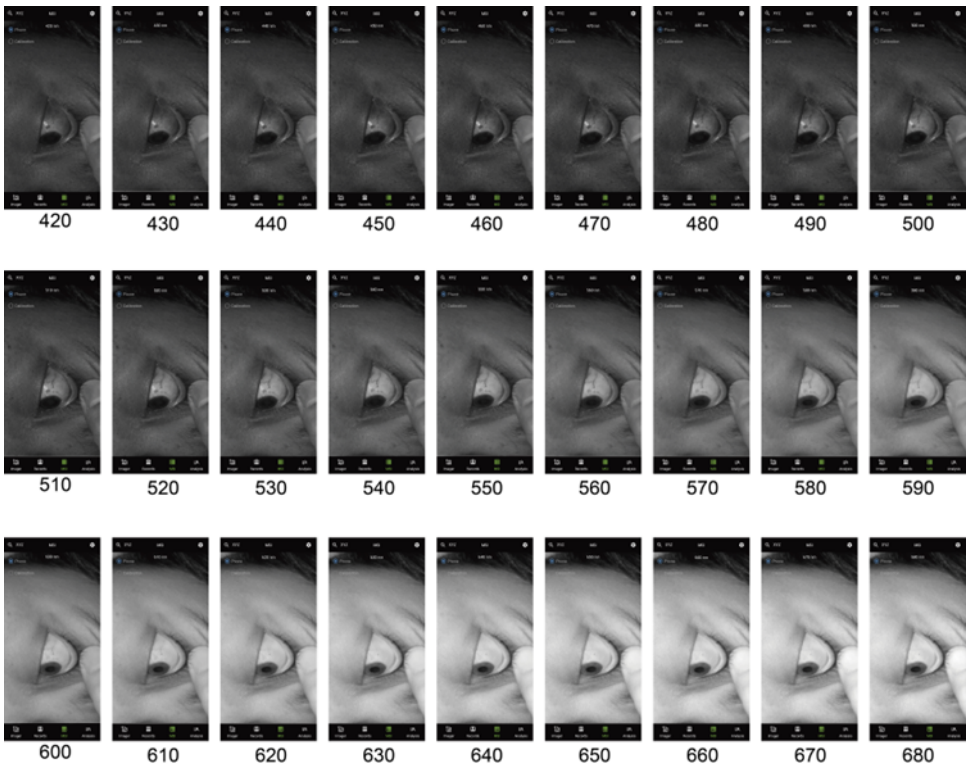

Fig. S4. The grayscale spectral images at wavelengths from 420 to 680 nm presented in the "MSI" fragment. The images can be checked by scrolling the screen, the wavelength would be accordingly labeled on the image. Please also see Visualization 2 (Movie S2.mp4).

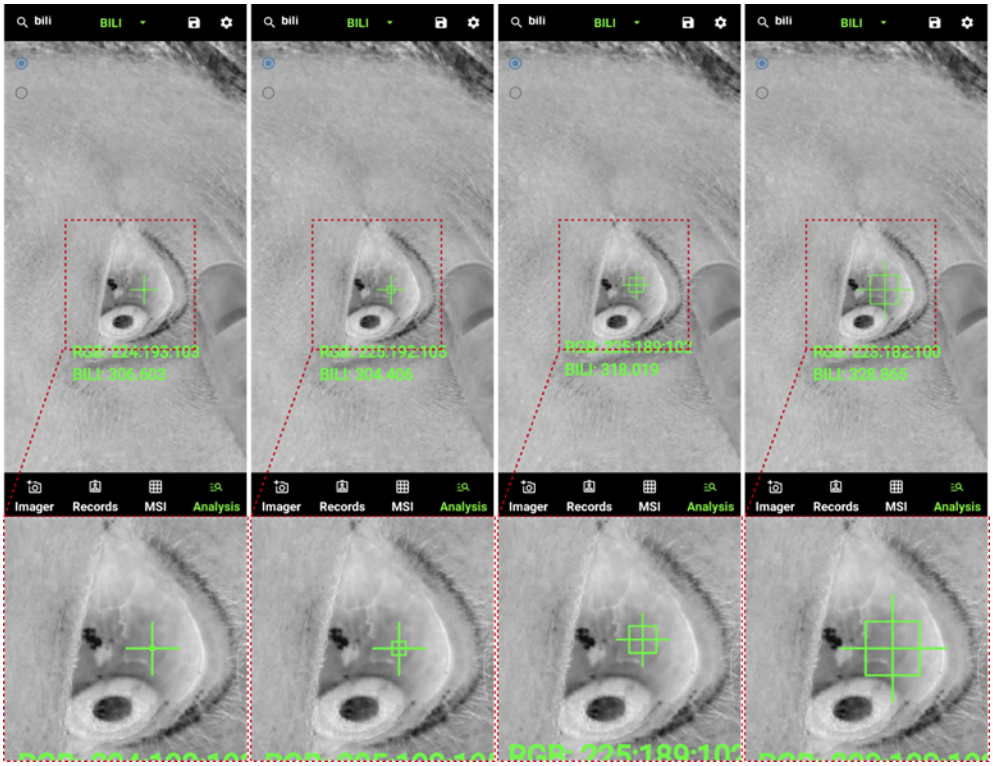

Fig. S5. The size of ROI can be set up in the “AVERAGE PIXELS”. Interfaces from the left to the right were under the setting of “8*8”, “32*32”, “64*64” and “128*128”, respectively.

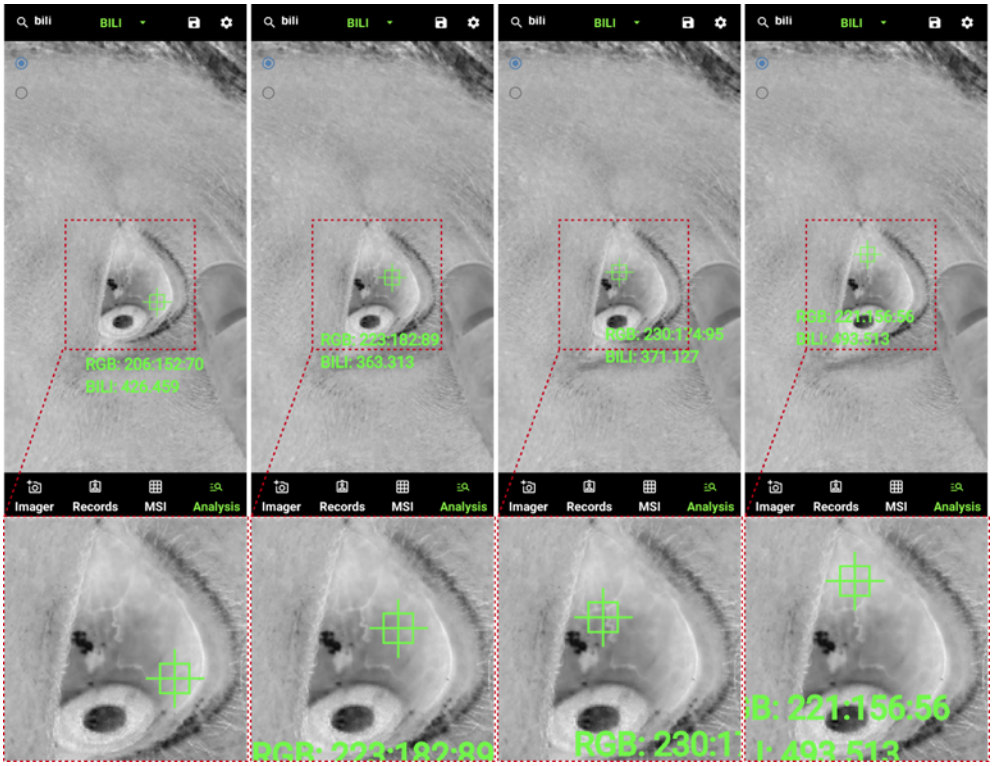

Fig. S6. Manual adjustments of the ROI position to sample different tissue regions by dragging the green marker. Please also see Visualization 3 (Movie S3.mp4).

Section 2. Accuracy of spectral reconstruction using SpeCamX

Table S1. RMSE of reconstructed reflectance spectrums using SpeCamX in X-rite ColorChecker Digital SG.

2	0.033	0.040	0.041	0.034	0.048	0.028	0.046	0.021	0.059	0.049	0.026	0.083
3	0.043	0.039	0.025	0.039	0.043	0.046	0.035	0.048	0.025	0.047	0.048	0.046
4	0.042	0.013	0.045	0.044	0.086	0.034	0.035	0.078	0.025	0.019	0.034	0.053
5	0.035	0.058	0.047	0.030	0.025	0.033	0.028	0.013	0.026	0.042	0.036	0.049
6	0.022	0.044	0.054	0.017	0.041	0.016	0.029	0.045	0.018	0.031	0.039	0.042
7	0.020	0.025	0.045	0.040	0.018	0.029	0.025	0.055	0.049	0.025	0.074	0.077
8	0.051	0.033	0.041	0.045	0.045	0.025	0.024	0.041	0.042	0.028	0.047	0.015
9	0.016	0.029	0.019	0.013	0.035	0.045	0.063	0.047	0.051	0.044	0.016	0.053
	B	C	D	E	F	G	H	I	J	K	L	M

Section 3. Comparison of prediction performance between SAL and RGBL using ANN and SVM

Fig. S7A shows the predictions obtained by ANN-based regression models. In 320 cases, we realized a correlation between SpeCamX and clinical BBL with a R at 0.90 ($p<0.0001$) and 0.83 ($p<0.0001$) for SAL and RGBL models, respectively. Except for higher R, the SAL prediction band (red band) is also narrower than the RGBL prediction band (black band). From the Bland-Altman plots (Fig. S7B), we can also observe smaller prediction bias in SAL prediction. Given richer information provided with higher spectral resolution, the SAL model should also learn quicker than the RGBL model. To validate this point, we reduced the data feeding to test and compare the prediction performance as well. Fig. S7A show the prediction results while the subjects were reduced by randomly resampling 75% (n=240), 50% (n=160), 25% (n=80) of the whole 320 cases, respectively. The prediction bands of both SAL and RGBL widened when the data set size was decreased. However, the SAL prediction band kept its relative stability while the RGBL prediction band showed increased instability. This observation was quantifiably verified in their corresponding Bland-Altman plots (Fig. S7B). The limits of agreement (LOA) of SAL prediction changed from +122.71/-124.43 μmol/L to +149.66/-157.26 μmol/L when the case number decreases from 320 to 80, but the LOA of RGBL expanded from +161.28/-171.10 μmol/L to +236.29/-234.65 μmol/L. This difference indicates that SpeCamX-enabled SAL can achieve predictions with higher quality than RGBL when the data feeding is limited.

In the results of SVM-based regression models (Fig. S7C), the regression coefficient of SAL is significantly closer to one than that of RGBL, indicating SAL prediction is less biased. This observation has been validated by the Bland-Altman plots in Fig. S7D, where SAL produces much smaller bias (9.22) than RGBL (23.32). Except for bias, the width of LOA is also smaller in SAL. When less data was fed, SAL predictions are relatively more stable. However, these two indices of RGBL prediction increased by ~35% (13.08 μmol/L) and ~30% (151.10 μmol/L) with 12.5% (n=40) data feeding, respectively.

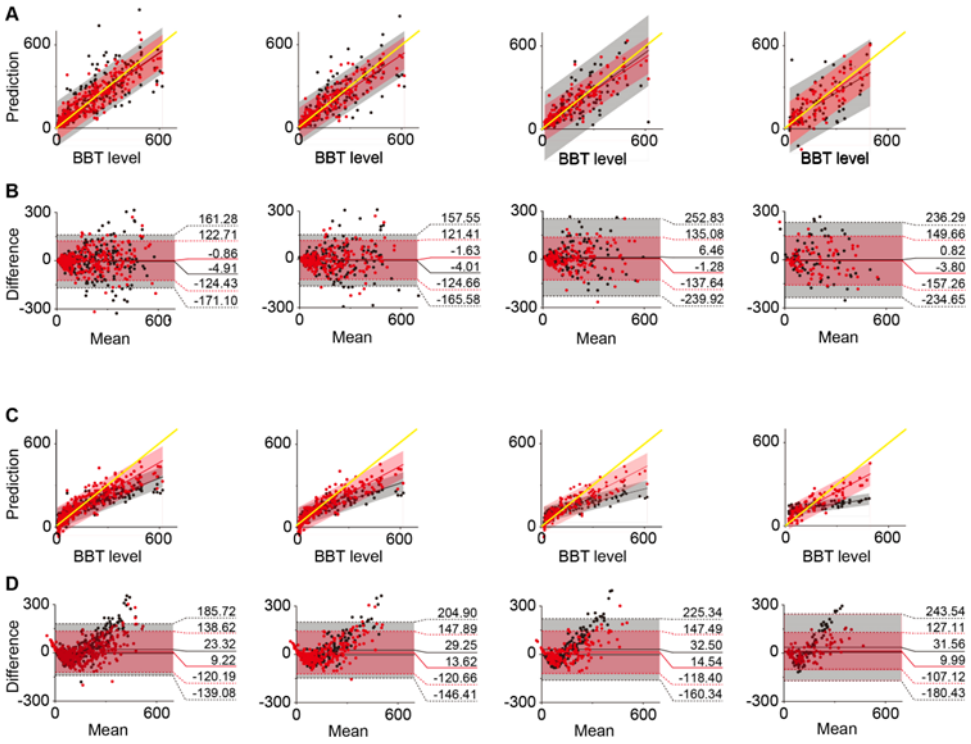

Fig. S7. Comparison of prediction performance between SAL and RGBL using ANN and SVM. (A, C) The relationship between BBL and predictions with SAL/RGBL using ANN and SVM, respectively. Black point: RGBL prediction; red point: SAL prediction; black area: 95% prediction band of RGBL prediction; red area: 95% prediction band of SAL prediction. (B, D) Bland-Altman plots of predictions with SAL and RGBL using KNN and RF, respectively. Black dotted line: 1.96 limits of agreement of RGBL prediction; red dotted line: 1.96 limits of agreement of SAL prediction; black line: mean error of RGBL prediction; red line: mean error of SAL prediction. All the groups with different sample sizes are randomly selected from the data pool of 320 patients. Units for all values are μmol/L. Resampling percentages from left to right: 100% (n=320); 75% (n=240); 50% (n=160); 25% (n=80).

Section 4. Comparison of prediction performance between SAL and RGBL using KNN and RF

Except for ANN and SVM, we also compared the SAL and RGBL predictions using KNN and RF algorithms (Fig. S8). In summary of these comparisons, SAL improves the prediction quality in varying degrees, especially with less data feeding. To illustrate this point clearer, we quantified the prediction performance of SAL and RGBL with data resampling percentage changing from 12.5% (n=40) to 100% (n=320) with a step width at 12.5% n=20). The R, MD and STD were then measured and presented as curves in Fig. S8. The evolution curves showed that the R of SAL always remained in high levels at 0.9 ($p<0.0001$), even when only 12.5% (n=20) of the data was used to train the model. On the contrary, the R of RGBL can be even lower than 0.6. In all methods except for SVM, the prediction biases of SAL are close to 0, smaller or at least comparable to RGBL predictions. In SVM, the bias of SAL is unneglectable, but also 55% (16.87±3.27 μmol/L) smaller than that of RGBL. The STD of MD in SAL slightly increase with smaller sample size but overall lower than 75 μmol/L, which is almost the best level the RGBL can reach.

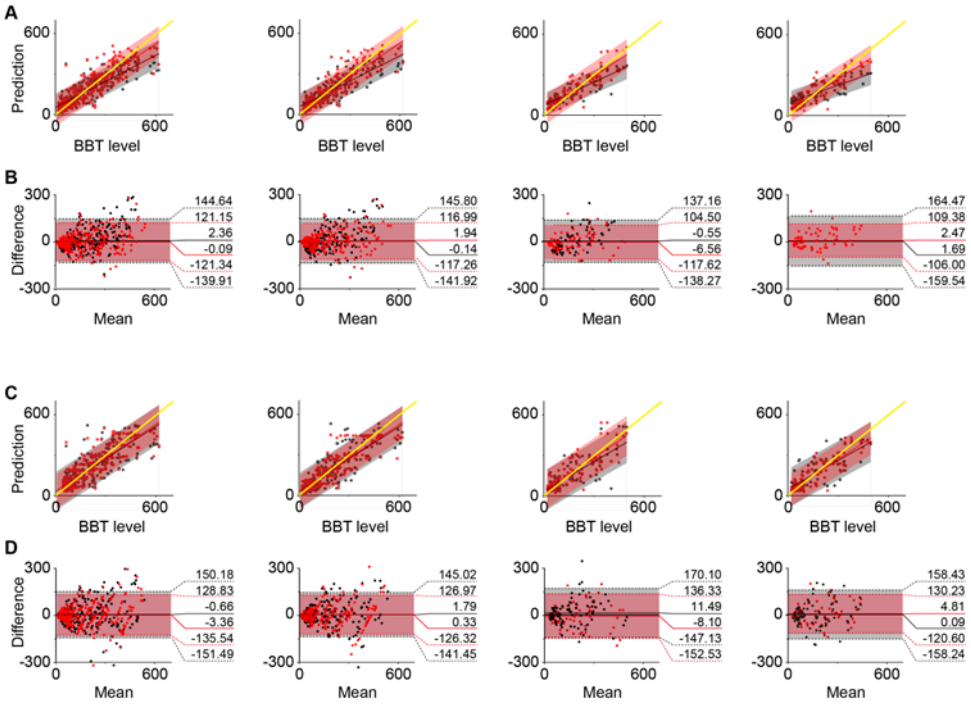

Fig. S8. Comparison of prediction performance between SAL and RGBL using KNN and RF. (A, C) The relationship between BBL and predictions with SAL/RGBL using KNN and RF, respectively. Black point: RGBL prediction; red point: SAL prediction; black area: 95% prediction band of RGBL prediction; red area: 95% prediction band of SAL prediction. (B, D) Bland-Altman plots of predictions with SAL and RGBL using KNN and RF, respectively. Black dotted line: 1.96 limits of agreement of RGBL prediction; red dotted line: 1.96 limits of agreement of SAL prediction; black line: mean error of RGBL prediction; red line: mean error of SAL prediction. All the groups with different sample sizes are randomly selected from the data pool of 320 patients. Units for all values are μmol/L. Resampling percentages from left to right: 100% (n=320); 75% (n=240); 50% (n=160); 25% (n=80).

Section 5. Stability of predictions in all groups using RGBL and SAL

Fig. S9 shows the bar graphs of prediction qualities in all groups with different sample sizes and algorithms using RGBL and SAL. The SAL owns lower standard deviations of R, MD and STD in all groups than RGBL, implying that SpeCamX-enabled prediction is more stable than conventional methods based on RGB photographs.

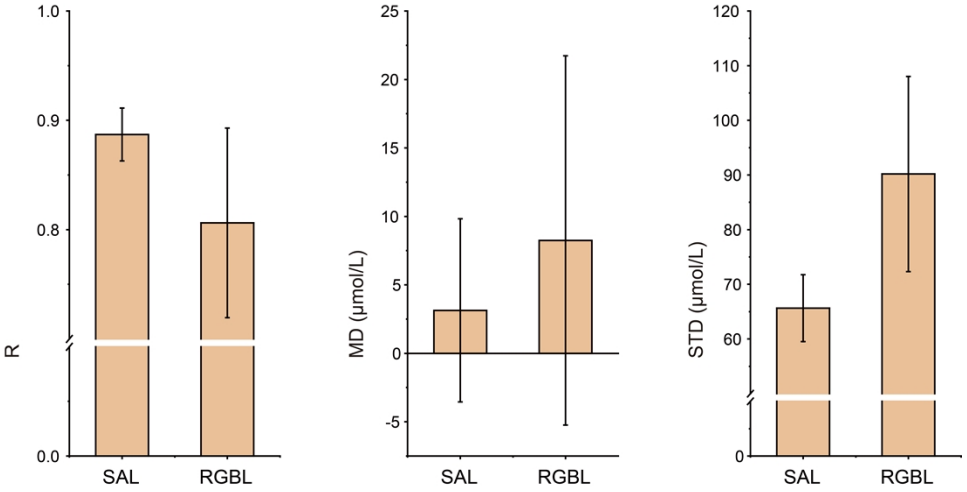

Fig. S9. Bar graphs of prediction qualities in all groups with different sample sizes and algorithms using RGBL and SAL. SAL-based predictions realized smaller STD than RGBL in R, MD and STD.